

## Unique cation-template three-dimensional hybrid material showing dielectric switchable response

Tie Zhang<sup>a</sup>, Shuang-Teng Song<sup>a</sup>, Hao-Nan Zhu<sup>a</sup>, Lu-Lu Chu<sup>a</sup>, Da-Wei Fu<sup>\*b</sup>, Yi Zhang<sup>\*a</sup>

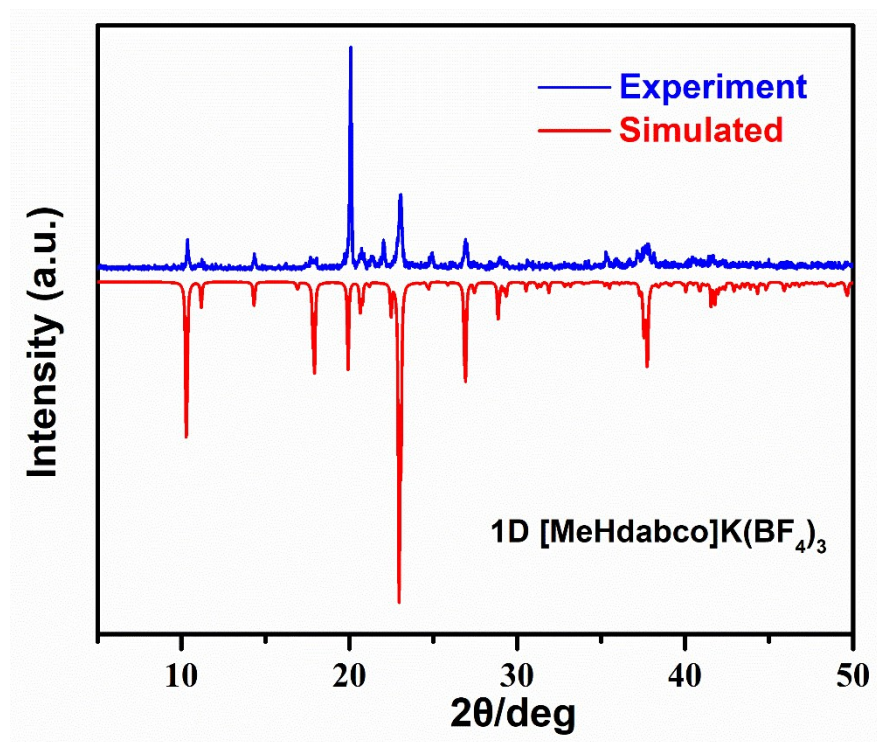


Fig.S1 The PXRD pattern of **1D** [MeHdabco]K(BF<sub>4</sub>)<sub>3</sub> (**MKBF-1**).

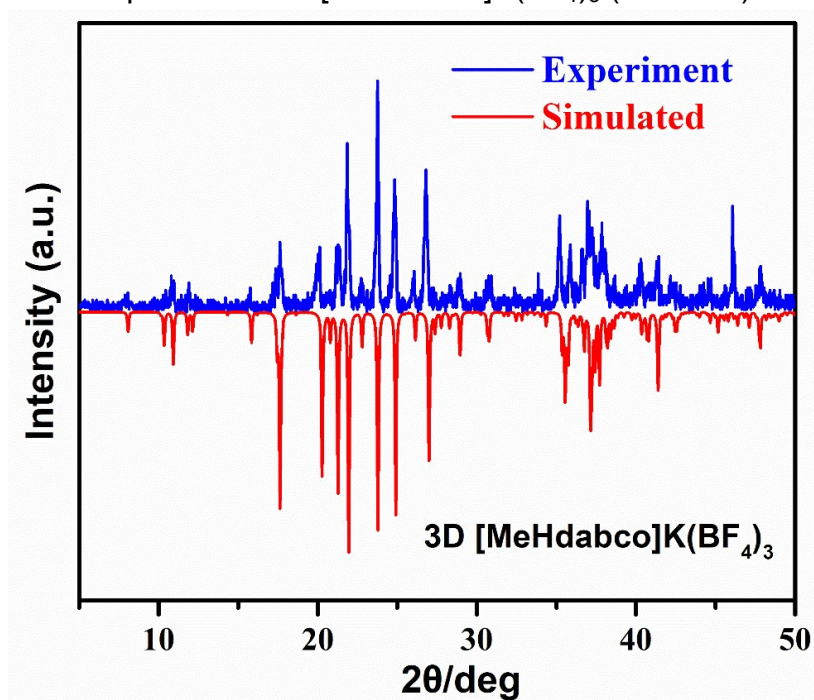


Fig. S2 The PXRD pattern of **3D** [MeHdabco]K(BF<sub>4</sub>)<sub>3</sub> (**MKBF-3**).

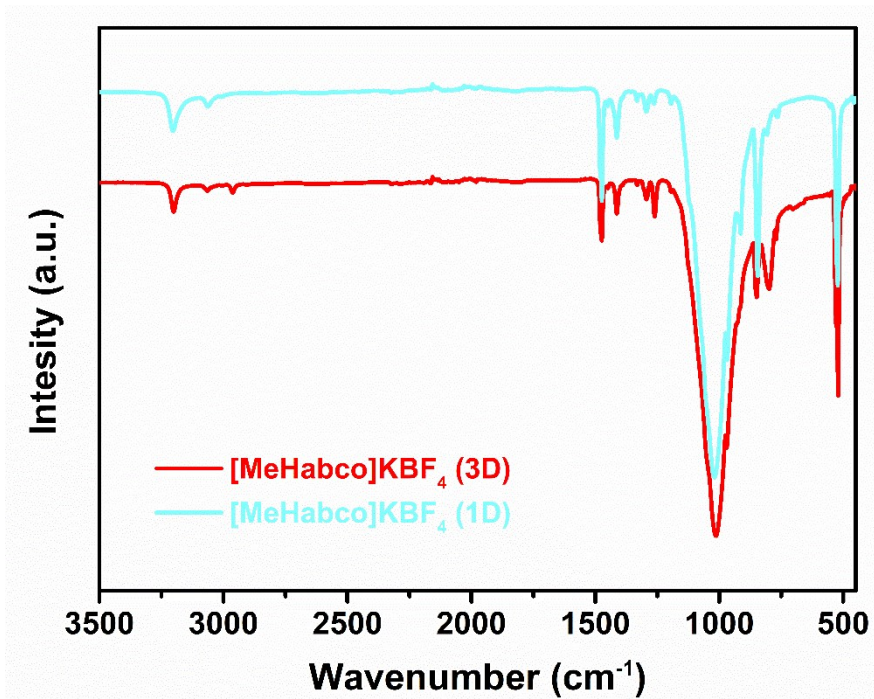


Fig. S3 The IR curves of Compound 1D [MeHdabco]K(BF<sub>4</sub>)<sub>3</sub> (MKBF-1) and 3D [MeHdabco]K(BF<sub>4</sub>)<sub>3</sub> (MKBF-3).

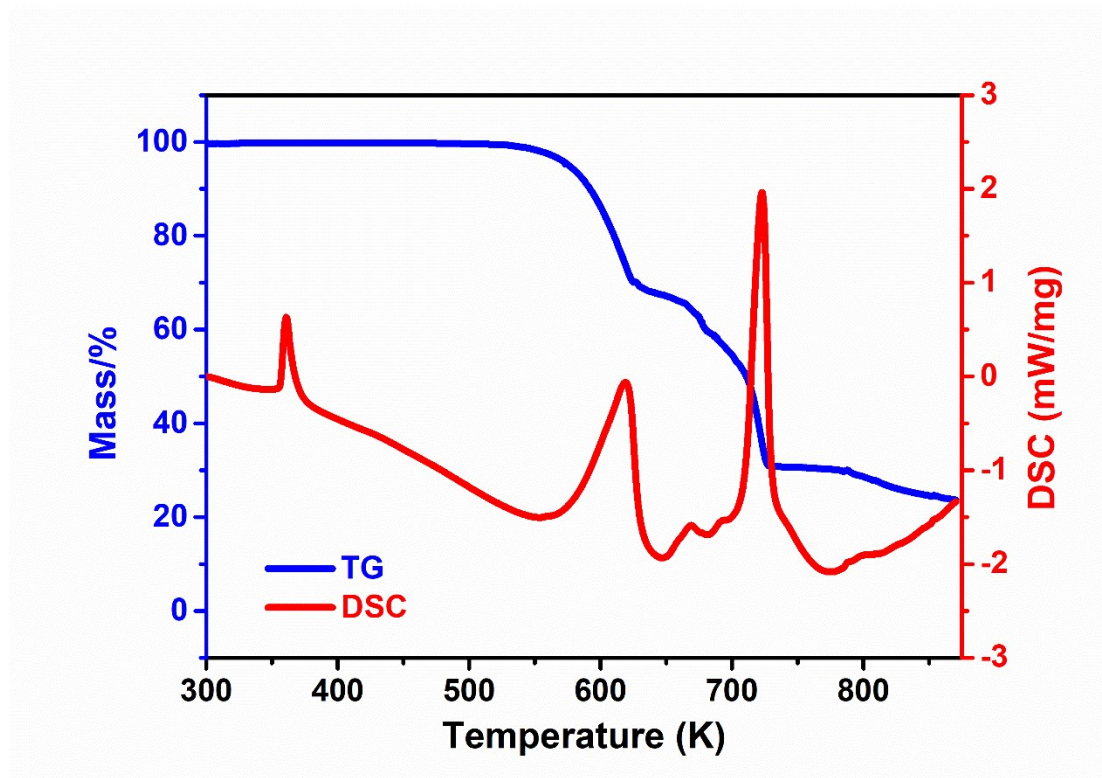


Fig. S4 The Thermogravimetric analysis (TGA) and DSC curves of MKBF-3.



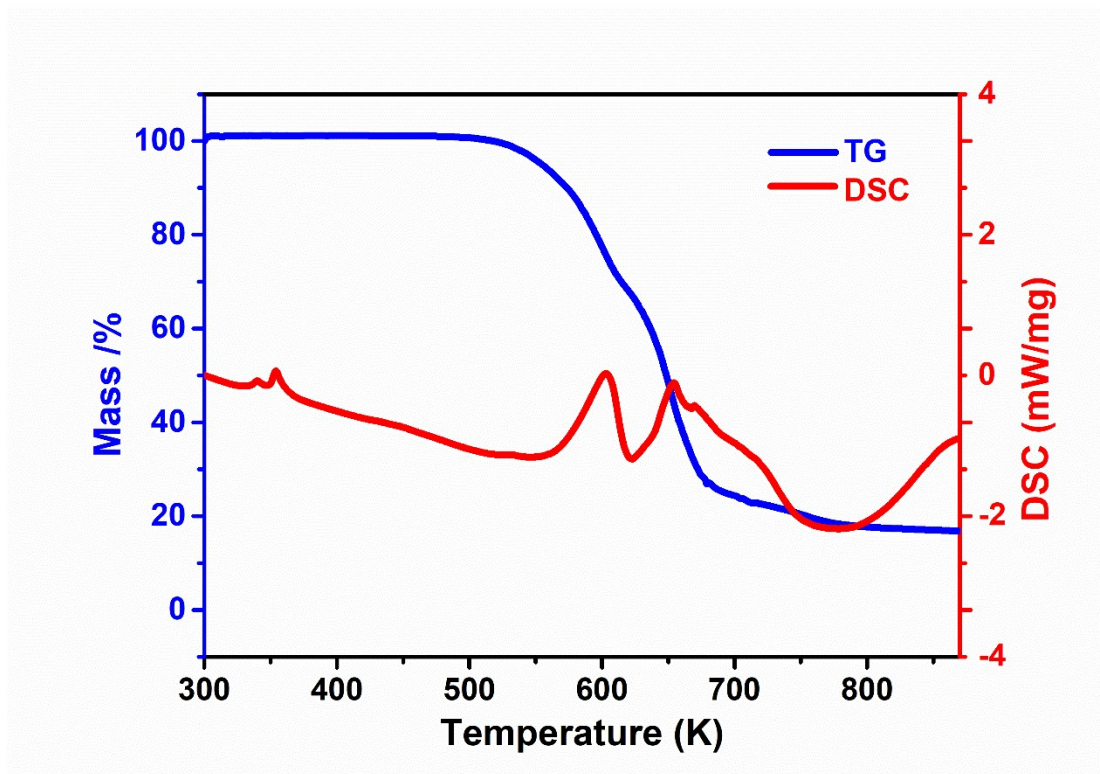


Fig. S5 The Thermogravimetric analysis (TGA) and DSC curves of **MKBF-1**.

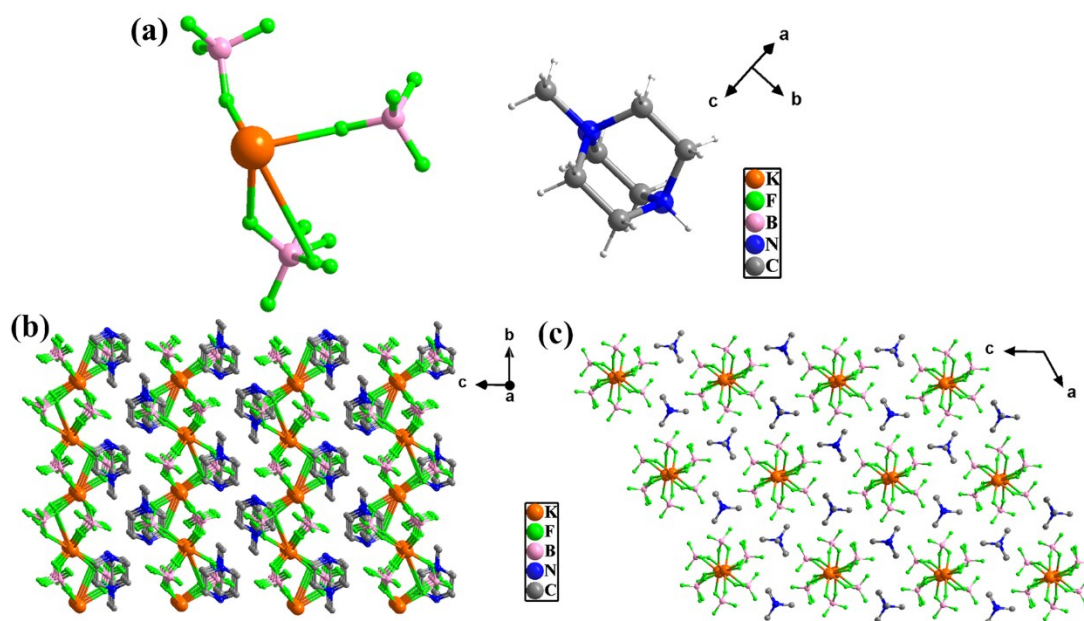


Fig. S6 (a) The molecular structure of compound **MKBF-1**. The packing structure of compound **MKBF-1** is viewed from a (b), and b (c) axis.

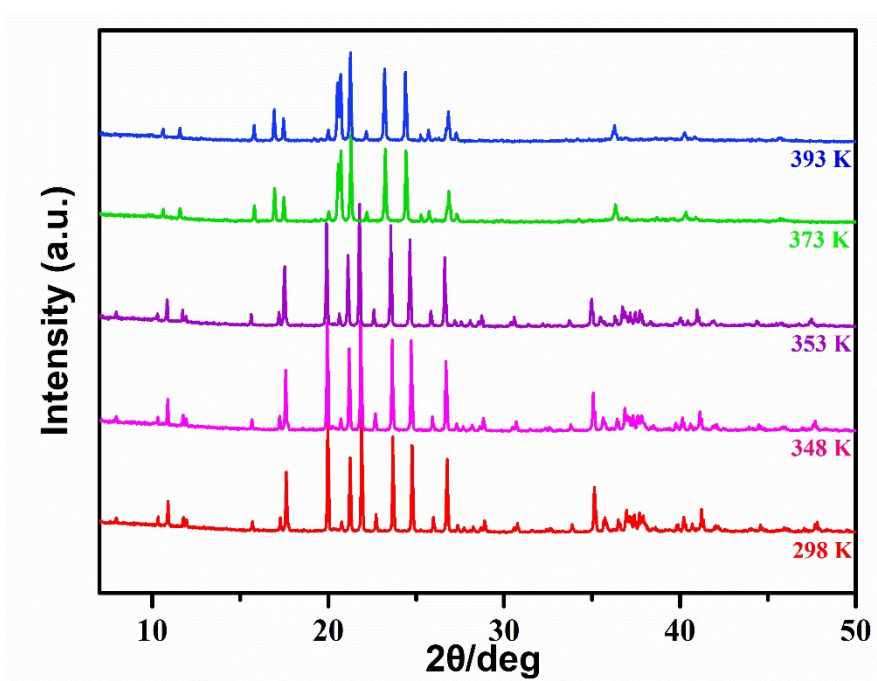


Fig. S7 Variable-temperature PXRD patterns of **MKBF-3** measured upon heating.

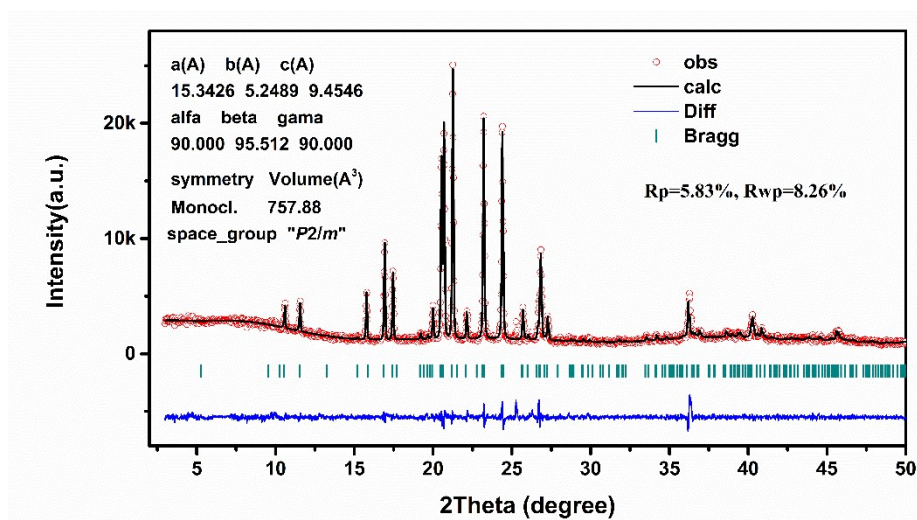


Fig. S8 The LeBail fit method refinement plot of **MKBF-3** structure at 393 K in high temperature phase state: experimental pattern (red line), calculated pattern (black line), difference profile (blue line). Through the LeBail fit refinements of the PXRD data (393 K), we obtained the monoclinic system (related lattice parameters are listed in insert figure).

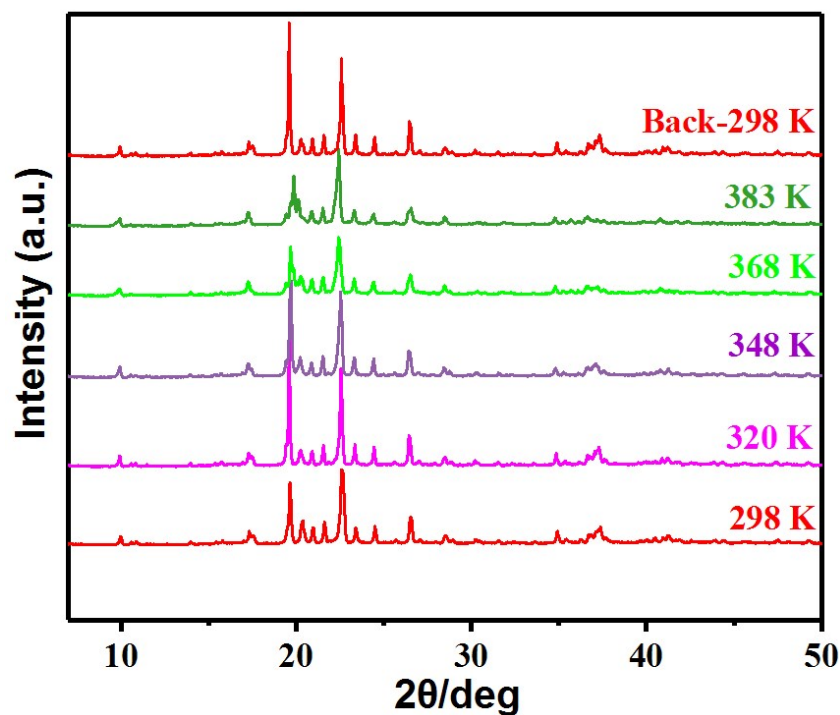


Fig. S9 Variable-temperature PXRD patterns of **MKBF-1** measured upon heating and back to 298 K.

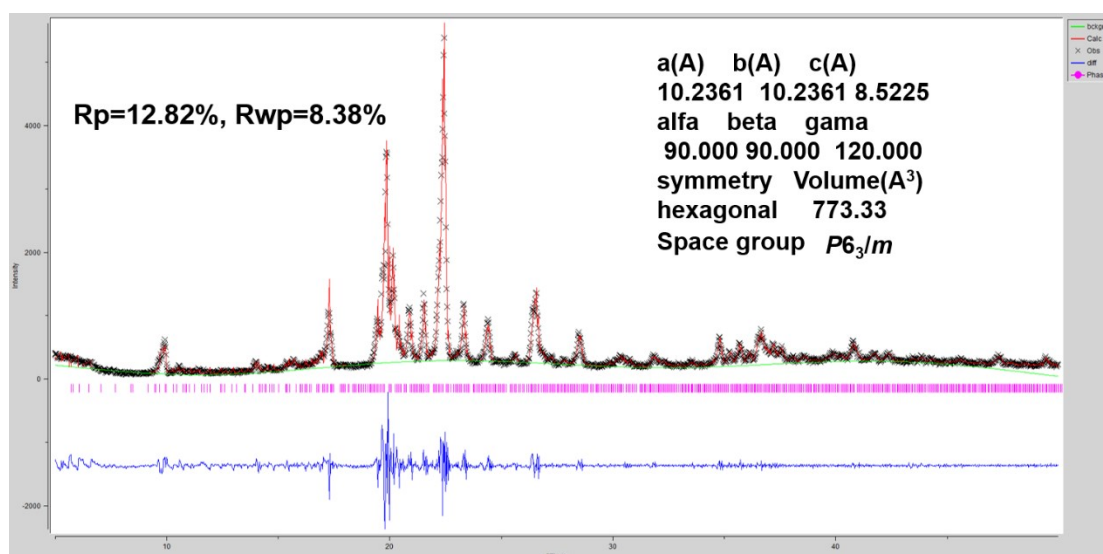


Fig. S10 The LeBail fit method refinement plot of **MKBF-1** structure at 383 K in high temperature phase state: experimental pattern (black line), calculated pattern (red line), difference profile (blue line) and background profile (green line). Through the LeBail fit refinements of the PXRD data (383 K), we obtained the hexagonal system (related lattice parameters are listed in insert figure).



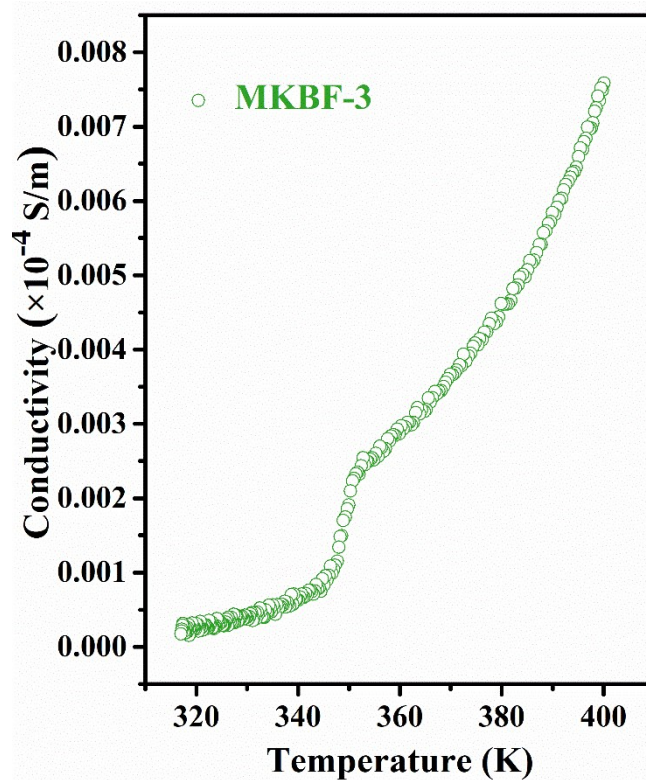


Fig. S11 The temperature dependence of the ac conductivity ( $\sigma$ ) for **MKBF-3**.

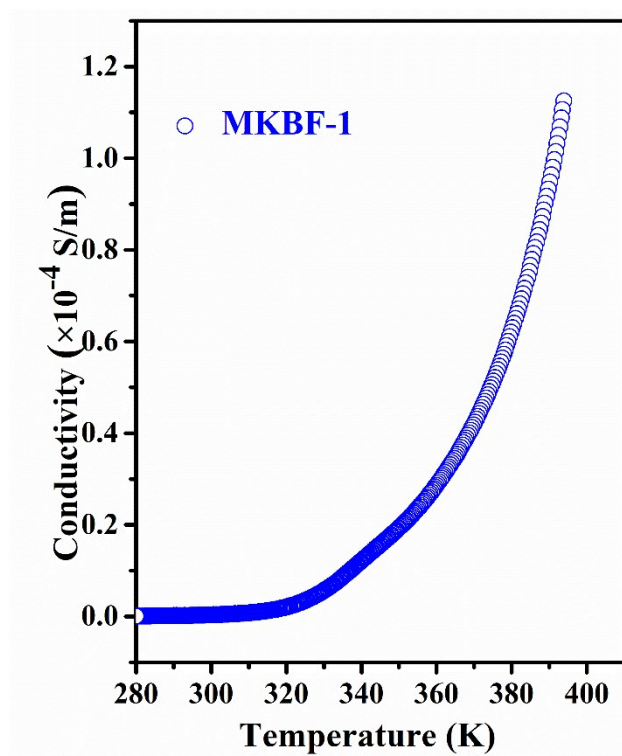


Fig. S12 The temperature dependence of the ac conductivity ( $\sigma$ ) for **MKBF-1**.

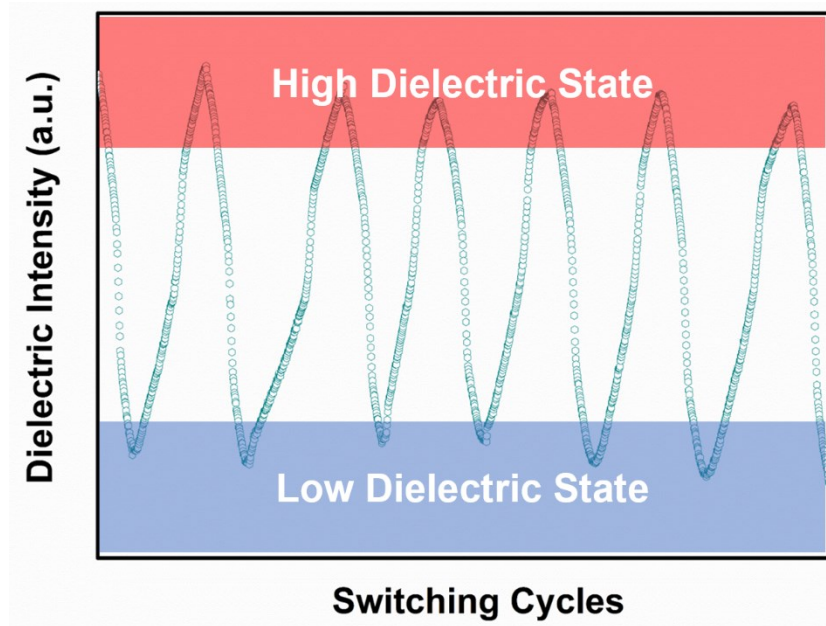


Fig. S13 Cycles of switching the high (ON) and low dielectric state (OFF) of  $\epsilon'$  at 1000 kHz over time for **MKBF-3**.

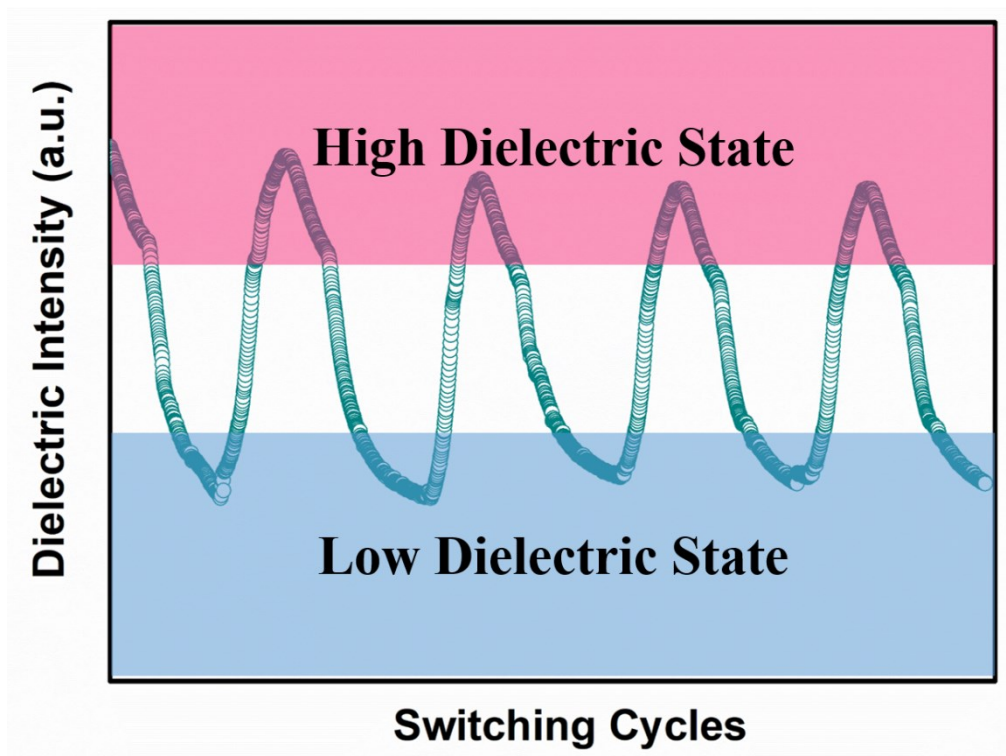


Fig. S14 Cycles of switching the high (ON) and low dielectric state (OFF) of  $\epsilon'$  at 1000 kHz over time for **MKBF-1**.

**Table S1.** Crystal data and structure refinements of compound **MKBF-1** and **MKBF-3**.

Compounds	MKBF-1	MKBF-3
<b>Empirical formula</b>	C <sub>7</sub> H <sub>16</sub> B <sub>3</sub> F <sub>12</sub> N <sub>2</sub> K	C <sub>35</sub> H <sub>80</sub> B <sub>15</sub> F <sub>60</sub> K <sub>5</sub> N <sub>10</sub>
<b>Formula weight</b>	427.75	2138.61
<b>Temperature(K)</b>	293	300
<b>Crystal system</b>	Monoclinic	hexagonal
<b>Space group</b>	<i>P</i> 2 <sub>1</sub> / <i>c</i>	<i>P</i> 6 <sub>3</sub> / <i>m</i>
<b><i>a</i>/ Å</b>	9.8794 (4)	10.0564(3)
<b><i>b</i>/ Å</b>	8.9060 (4)	10.0564(3)
<b><i>c</i>/ Å</b>	19.7825 (8)	43.757(6)
<b><i>α</i>°</b>	90	90
<b><i>β</i>°</b>	119.608 (3)	90
<b><i>γ</i>°</b>	90	120
<b>Volume(Å<sup>3</sup>)</b>	1579.36(10)	3832.3(6)
<b>Radiation type</b>	Mo-Ka	Mo-Ka
<b>Absorption correction</b>	Semi-empirical	Semi-empirical
<b>D<sub>calc</sub> / g cm<sup>-3</sup></b>	1.878	1.839
<b>F(000)</b>	856.0	2108
<b>Completeness to <i>θ</i>(%)</b>	99.82	99.80
<b>GOF</b>	1.16	1.059
<b>R<sub>1</sub><sup>[a]</sup>[<i>I</i> &gt; 2σ(<i>I</i>)]</b>	0.142	0.0641
<b>wR<sub>2</sub><sup>[b]</sup>[<i>I</i> &gt; 2σ(<i>I</i>)]</b>	0.299	0.1833

$$^{[a]}R_1 = \sum ||F_o| - |F_c|| / \sum |F_o|, ^{[b]}wR_2 = [\sum w(F_o^2 - F_c^2)^2] / \sum w(F_o^2)^2]^{1/2}$$

**Table S2.** Selected bond lengths [Å] for compound **MKBF-1** and **MKBF-3**.

Compounds	Bond lengths (Å)	
<b>MKBF-1</b>	K1—F4 <sup>i</sup>	2.244 (13)
	K1—F12	2.285 (8)
	K1—F16	2.294 (6)
	K1—F4 <sup>i</sup>	2.370 (13)
	K1—F2	2.347 (6)
	K1—F8	2.359 (6)
<b>MKBF-3</b>	K1—F4	2.801 (3)
	K1—F5	2.882 (3)
	K1—F6	3.108 (3)
	K1—F4 <sup>vii</sup>	2.801 (3)



---

K1—F4 <sup>viii</sup>	2.801 (3)
K1—F5 <sup>vii</sup>	2.882 (3)
K1—F5 <sup>viii</sup>	2.882 (3)
K1—F6 <sup>vii</sup>	3.108 (3)
K1—F6 <sup>viii</sup>	3.108 (3)
K3—F7	2.954 (3)
K3—F8	3.116 (3)
K3—F9	2.966 (3)
K3—F12	2.871 (2)
K3—F12 <sup>ii</sup>	2.871 (2)
K3—F12 <sup>vi</sup>	2.871 (2)
K3—F7 <sup>ix</sup>	2.954 (3)
K3—F7 <sup>vi</sup>	2.954 (3)
K3—F9 <sup>vi</sup>	2.966 (3)
K3—F9 <sup>ix</sup>	2.966 (3)
K3—F8 <sup>ix</sup>	3.116 (3)
K3—F8 <sup>vi</sup>	3.116 (3)
K5—F2	2.784 (2)
K5—F2 <sup>x</sup>	2.784 (2)
K5—F2 <sup>xi</sup>	2.784 (2)
K5—F2 <sup>xii</sup>	2.784 (2)
K5—F2 <sup>xiii</sup>	2.784 (2)
K5—F2 <sup>xiv</sup>	2.784 (2)
K5—F1 <sup>xiii</sup>	3.293 (2)
K5—F1 <sup>xii</sup>	3.293 (2)
K5—F1 <sup>xi</sup>	3.293 (2)
K5—F1 <sup>x</sup>	3.293 (2)
K5—F1 <sup>xiv</sup>	3.293 (2)

---

**MKBF-1:** (i)  $-x, y-1/2, -z+1/2$ ; **MKBF-3:** (i)  $x, y, -z+1/2$ ; (ii)  $-x+y, -x+1, -z+1/2$ ; (iii)  $-x+y+1, -x+1, z$ ; (iv)  $-y+1, x-y, z$ ; (v)  $-x+y+1, -x+1, -z+1/2$ ; (vi)  $-y+1, x-y+1, z$ ; (vii)  $-x+y-1, -x, z$ ; (viii)  $-y, x-y+1, z$ ; (ix)  $-x+y, -x+1, z$ ; (x)  $x-y, x, -z$ ; (xi)  $-x+y, -x, z$ ; (xii)  $y, -x+y, -z$ ; (xiii)  $-y, x-y, z$ ; (xiv)  $-x, -y, -z$ .

**Table S3.** Enthalpy and Entropy Changes of **MKBF-1** and **MKBF-3** from DSC Data.

	$\Delta H(\text{kJ}\cdot\text{mol}^{-1})$	$\Delta S(\text{J}\cdot\text{mol}^{-1}\cdot\text{K}^{-1})$	$N$
<b>MKBF-1</b>	1.42	4.16	1.6
	5.38	15.15	6.2
<b>MKBF-3</b>	37.062	103.24	247211.62